Active Sensor Fault Tolerant Output Feedback Tracking Control for Wind Turbine Systems via T-S Model

Montadher Sami Shaker[*] and Ron J. Patton[**]

[*]*Department of Electrical Engineering, University of Technology, Baghdad, Iraq*

e-mail: m.s.shaker@uotechnology.edu.iq

[**]*Department of Engineering, University of Hull, Hull HU6 7RX, UK*
e-mail: r.j.patton@hull.ac.uk ;

Abstract: This paper presents a new approach to active sensor fault tolerant tracking control (FTTC) for offshore wind turbine (OWT) described via Takagi-Sugeno (T-S) multiple models. The FTTC strategy is designed in such way that aims to maintaining nominal wind turbine controller without change in both fault and fault-free cases. This is achieved by inserting T-S proportional state estimators augmented with proportional and integral feedback (PPI) fault estimators to be capable to estimate different generator and rotor speed sensors fault for compensation purposes. Due to the dependency of the FTTC strategy on the fault estimation the designed observer has the capability to estimate a wide range of time varying fault signal. Moreover, the robustness of the observer against the difference between the anemometer wind speed measurement and the immeasurable effective wind speed signal has been taken into account. The corrected measurements fed to a T-S fuzzy dynamic output feedback controller (TSDOFC) designed to track the desired trajectory. The stability proof with H_∞ performance and D-stability constraints is formulated as a Linear Matrix Inequality (LMI) problem. The strategy is illustrated using a non-linear benchmark system model of a wind turbine offered within a competition led by the companies Mathworks and KK-Electronic.

Keywords: Active fault tolerant control, Fault estimation, Tracking control, T-S fuzzy systems, Dynamic output feedback control, LMI formulation, Wind turbine control.

1. Introduction

Owing to inherent limitations in different kinds of the well-known fossil fuel and nuclear energy sources, e.g. carbon footprint, rapidly increasing fuel prices or probability of catastrophic effects of nuclear station malfunction, the last two decades have witnessed a rapid growth in the use of wind energy. Although, it is considered a promising source of energy, depending on naturally generated wind forces, there are several very significant challenges to efficient wind energy conversion for electrical power transformation (Marden, Ruben and Pao, 2013, Odgaard, Stoustrup and Kinnaert, 2013).

Wind turbine systems demand a high degree of reliability and availability (sustainability) and at the same time are characterised by expensive and safety critical maintenance work (Verbruggen, 2003). The recently developed OWTs are foremost examples since OWT site accessibility and system availability is not always ensured during or soon after malfunctions, primarily due to changing weather conditions. Hence, the main challenges for the deployment of wind turbine systems are to maximise the amount of good quality electrical power extracted from wind energy over a significantly wide range of weather conditions and minimize both manufacturing and maintenance costs. To maximise the amount of the annual power production an increase in wind turbine size has been suggested, another opportunity is the development of a variable speed wind turbine which enhances both quality and the amount of the power production compared with the fixed speed wind turbines (Bianchi, de Battista and Mantz, 2007). Furthermore, to reduce the effects of obstacles and roughness of terrain that increase wind force turbulence, OWT are currently being developed and installed (Stewart and Lackner, 2013).

In the last years, a number of publications consider the effect of wind turbines malfunction is noticed with focusing on designing fault tolerant control (FTC) (Sloth, Esbensen and Stoustrup, 2011, Kamal, Aitouche, Ghorbani and Bayart, 2012, Sami and Patton, 2012b, Sami and Patton, 2012a, Badihi, Zhang and Hong, 2013, Jain, Yame and Sauter, 2013, Odgaard, Stoustrup and Kinnaert, 2013, Simani and Castaldi, 2013a, Simani and Castaldi, 2013b) and fault monitoring systems (Amirat et al., 2009, Hameed et al., 2009, Wei and Liu, 2010, Johnson and Fleming, 2011, Djurovic, Crabtree, Tavner and Smith, 2012). In (Sloth, Esbensen and Stoustrup, 2011), the authors proposed linear parameter-varying FTC systems for pitch actuator faults occurring in the full load operation. In (Kamal, Aitouche, Ghorbani and Bayart, 2012) a T-S fuzzy observer-based FTC design is proposed to achieve maximization of the power extraction in the presence of generator sensor fault without taking into account the trade-off between the tracking of the optimal signal and the loads induced in the drive train due to exact tracking of optimal signal. (Jain, Yame and Sauter, 2013) presents a real-time projection-based approach to tolerate faults occurring in a wind turbine system. In (Sami and Patton, 2012b, Sami and Patton, 2012a) the robustness of sliding mode control have been utilized to design FTC for OWT. (Badihi, Zhang and Hong, 2013) presents an approach in designing a fault detection and diagnosis (FDD) and FTC scheme for a wind turbine using fuzzy modelling and control. (Simani and Castaldi, 2013a) proposed a fault tolerant controller to accommodate actuator fault using the on-line fault estimate signal generated by an adaptive filter. The fuzzy approach to wind turbine controller design in the presence of modelling and measurement errors has also been proposed in (Simani and Castaldi, 2013b)

Generally, wind turbines have non-linear aerodynamics and this limits the use of a linear systems approach without due care to robustness issues. Furthermore, wind turbines have a stochastic and uncontrollable driving force as input in the form of wind speed. This, together with overall system nonlinearity limits the ability of linear control strategies to satisfy the control objectives. Hence, an increase in interest in controlling wind turbines through nonlinear control methods has been noticed in the last years to handle the nonlinearity of the turbine aerodynamics. This is achieved either through the use of nonlinear models directly in the design (Sami and Patton, 2012b, Sami and Patton, 2012a) or through the use of multiple-model approaches (Sloth, Esbensen and Stoustrup, 2011, Kamal, Aitouche, Ghorbani and Bayart, 2012, Badihi, Zhang and Hong, 2013) .

This paper focuses on the design of FTTC dedicated to optimise the captured wind energy. Based on the wind turbine T-S fuzzy model, a TSDOFC is designed to achieve the required tracking of the optimal rotor speed (ω_{ropt}) and the reduction of loads affecting the drive-train through minimising the L_2 norm of the wind variation on the torsion angle of the drive train. The FTTC is achieved by hiding the effects of different generator and rotor sensors fault from the controller inputs through the insertion of the PPI observer (PPIO) capable of handling the case of time-varying fault signals. The proposed strategy overcomes the dependence and limitation of requiring full state measurements. The technique also focuses on minimizing the difficulties of designing observer based control systems that require special pole placement conditions since these conditions cannot hold perfectly in the multiple model framework due to global stability constraints. The design also locates the controller and observer poles of each T-S model system to lie within a disc region of the complex plane. Finally, the design is formulated as a linear matrix inequality problem that can be solved easily using MATLAB software. The simulation results are based using a non-linear benchmark system model of a wind turbine offered within a competition led by the companies Mathworks and KK-Electronic (Odgaard, Stoustrup and Kinnaert, 2009, Odgaard, Stoustrup and Kinnaert, 2013).

2. The proposed active FTTC

Generally, active FTC (AFTC) systems are designed to handle the occurrence of system faults on-line by using fault estimation/compensation methods, adaptive control or controller reconfiguration mechanisms. All AFTC methods involve some advantages and disadvantages. The operation philosophy of adaptive control fits very well with the AFTC approach. This is due to the ability of adaptive control systems to adjust controller parameters on-line based on measured signals. Clearly, the use of adaptive control methods as an approach to AFTC obviates the need for fault detection and diagnosis (FDD) unit. However, in this method, sensor faults represent the most challenging fault scenario for AFTC and have rarely been considered in fault tolerant adaptive control methods. For example, output feedback adaptive tracking control can tolerate actuator and/or system faults, whereas, if sensor faults have occurred the adaptation will force the faulty output to follow the reference signals and hence the control signal will no longer be suitable for the system under control. The controller reconfiguration approach can handle more general faults and/or failure cases through either off-

line or on-line variation of the structure and/or the parameters of the controller based on the information delivered from an FDD unit. However, the main challenge of this method is that the time required to reconfigure the control system must be as low as possible. In fact, this is very important in practice where the time windows during which the system remains stabilisable in the presence of a fault are very short. This is especially the case for unstable open-loop systems, e.g. the unstable double inverted pendulum example (Niemann and Stoustrup, 2005). On the other hand, as an extension to the use of FDD base control reconfiguration, the estimation and compensation approach to FTC is based on the computation of fault estimates and a mechanism to compensate these fault effects by the addition of a new compensating signal to the nominal control input or faulty measured output. Clearly, this approach obviates the need for residual evaluation and parameter identification steps that required for FDD based FTC and hence requires no time consuming algorithms for maintaining the performance of the nominal system control law. Moreover, the inability of the adaptive control-based FTC to tolerate sensor faults means that fault estimation and compensation represents the all round most appropriate method for the sensor fault case of FTC.

Within the framework of estimation and compensation, this section present the structure of the proposed FTTC strategy for OWT control problems based on robust fault estimation and compensation of rotor rotational speed sensor faults $\hat{f}_{sr}$ and/or generator rotational speed sensor faults $\hat{f}_{sg}$ whilst maintaining the performance and stability of the nominal control system during both faulty and fault-free cases. It is clear from the architecture shown in Fig. 1, the proposed FTTC scheme is based on the combination of (a) robust TSDOFC and (b) estimates of the $\hat{f}_{sr}$ and/or $\hat{f}_{sg}$ via the T-S fuzzy PPIO. This strategy can be considered as a "fault-hiding" approach to FTC where the main aim of fault-hiding is to maintain the same controller in both faulty and fault-free system cases. Specifically, the T-S fuzzy PPIO will hide sensor faults through fault estimation and compensation so that the TSDOFC always receives the fault free measurements.

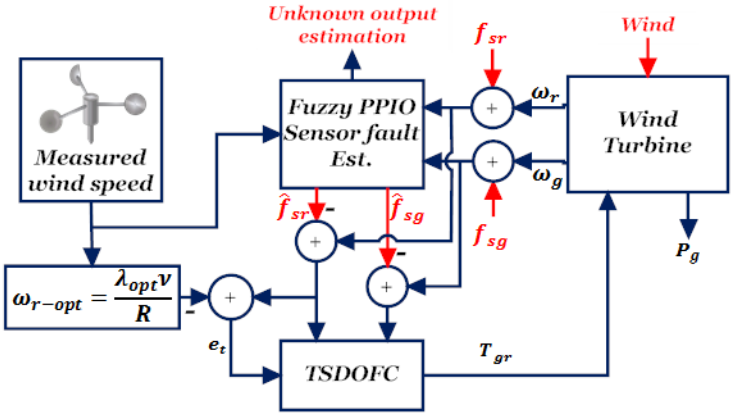

Fig. 1: Active sensor FTTC scheme

It should be noted that the T-S fuzzy model consists of local linear input-output relations of the nonlinear system. The overall fuzzy model is achieved by connecting the local linear models by membership functions yielding the global model of the system. It is important to note that a T-S fuzzy controller is a model-based control approach. The procedure of designing T-S fuzzy controller and/or T-S fuzzy observer should start from deriving the T-S fuzzy model. Hence, the next section presents the nonlinear model of the wind turbine and the derivation of its corresponding T-S model.

3. Wind turbine modelling

A wind turbine model is obtained by combining the constituent component subsystem models that together make up the overall wind turbine dynamics. The aerodynamic torque (T_a) represents the source of nonlinear nature of wind turbine which in turn depends on the rotor speed ω_r , the blade pitch angle β and the effective rotor wind speed v. The aerodynamic power captured by the rotor is given by

$$P_{cap} = \frac{1}{2}\rho\pi R^2 C_p(\lambda,\beta)v^3 \tag{1}$$

where ρ is the air density, R is the radius of the rotor, and C_p is the power coefficient that depends on the β and the tip-speed-ratio (λ) (TSR) which defined as

$$\lambda = \frac{\omega_r R}{v} \tag{2}$$

The aerodynamic torque is

$$T_a = \frac{1}{2}\rho\pi R^3 C_q(\lambda,\beta)v^2 \tag{3}$$

where $C_q = \frac{C_p}{\lambda}$ is the torque coefficient.

The drive train is responsible for gearing up the rotor rotational speed to a higher generator rotational speed. The drive train model includes low and high speed shafts linked together by a gearbox modelled as a gear ratio. The state space model of the wind turbine drive train in the form:

$$\begin{bmatrix}\dot{\omega}_r\\ \dot{\omega}_g\\ \dot{\theta}_\Delta\end{bmatrix} = \begin{bmatrix} -\frac{(B_{ls}+B_r)}{Jr} & \frac{B_{ls}}{n_g Jr} & -\frac{K_{ls}}{Jr} \\ \frac{B_{ls}}{n_g J_g} & -\frac{(B_{ls}+n_g B_g)}{n_g^2 J_g} & \frac{K_{ls}}{n_g J_g} \\ 1 & -\frac{1}{n_g} & 0 \end{bmatrix}\begin{bmatrix}\omega_r\\ \omega_g\\ \theta_\Delta\end{bmatrix} + \begin{bmatrix}\frac{1}{J_r} & 0\\ 0 & -\frac{1}{J_g}\\ 0 & 0\end{bmatrix}\begin{bmatrix}T_a\\ T_g\end{bmatrix} \tag{4}$$

Where J_r is the rotor inertia, B_r is the rotor external damping, J_g is the generator inertia, ω_g and T_g is the generator speed and torque, B_g is the generator external damping, n_g is the gearbox ratio, and θ_Δ is the torsion angle.

The electrical system in the wind turbine and the electrical system controllers are much faster than the frequency range used in the benchmark model. Hence, the electrical system is given by the following linear relation

$$\dot{T}_g = -\frac{1}{\tau_g}T_g + \frac{1}{\tau_g}T_{gr} \tag{5}$$

Where T_{gr} is the reference generator torque signal and $\tau_g$is the time constant. Finally, the hydraulic pitch system is modelled as a closed-loop transfer function between the measured pitch angle β and its reference β_r:

$$\beta = \frac{\omega_n^2}{s^2 + 2\zeta\omega_n s + \omega_n^2}\beta_r \tag{6}$$

where ζ is the damping factor and ω_n is the natural frequency. For the three blade wind turbine system, a transfer function is associated with each of the three pitch systems. In cases of no fault the damping factors are assumed equal.

3-1. The state space model

For controller design purposes the state space model of wind turbine is presented in this subsection. The nonlinear model of a wind turbine is established by combining the individual systems given in Eqs. (3-6). However, it is clear that the main source of nonlinearity is the aerodynamic subsystem which is usually linearized in order to predict its effects on all model states. Hence, the state space model of wind turbine is given as:

$$\left.\begin{aligned}\dot{x} &= Ax(t) + Bu + Ev\\ y &= Cx(t)\end{aligned}\right\} \tag{7}$$

where

$$A=\begin{bmatrix} -\frac{1}{\tau_g} & 0 & 0 & 0 & 0 & 0 \\ 0 & 0 & I & 0 & 0 & 0 \\ 0 & -\omega_n^2 I & -2\zeta\omega_n I & 0 & 0 & 0 \\ 0 & \frac{1}{J_r}\frac{\partial T_a}{\partial \beta} & 0 & -\frac{(B_{dt}+B_r)}{J_r}+\frac{1}{J_r}\frac{\partial T_a}{\partial \omega_r} & \frac{B_{dt}}{n_g J_r} & -\frac{K_{dt}}{J_r} \\ -\frac{1}{J_g} & 0 & 0 & \frac{B_{dt}}{n_g J_g} & -\frac{(B_{dt}+n_g B_g)}{n_g^2 J_g} & \frac{K_{dt}}{n_g J_g} \\ 0 & 0 & 0 & 1 & -\frac{1}{n_g} & 0 \end{bmatrix}$$

$$B=\begin{bmatrix} \frac{1}{\tau_g} & 0 \\ 0 & 0 \\ 0 & \omega_n^2 I \\ 0 & 0 \\ 0 & 0 \\ 0 & 0 \end{bmatrix}, E=\begin{bmatrix} 0 \\ 0 \\ 0 \\ \frac{1}{J_r}\frac{\partial T_a}{\partial v} \\ 0 \\ 0 \end{bmatrix}, C=\begin{bmatrix} 1 & 0 & 0 & 0 & 0 & 0 \\ 0 & 1 & 0 & 0 & 0 & 0 \\ 0 & 0 & 0 & 1 & 0 & 0 \\ 0 & 0 & 0 & 0 & 1 & 0 \end{bmatrix}, x=\begin{bmatrix} T_g \\ \beta \\ \dot{\beta} \\ \omega_r \\ \omega_g \\ \theta_\Delta \end{bmatrix}, u=\begin{bmatrix} T_{gr} \\ \\ \beta_r \end{bmatrix}$$

$$\frac{\partial T_a}{\partial \beta}=\frac{1}{2\omega_r}\rho A v^3\,\frac{\partial C_p}{\partial \beta}$$

$$\frac{\partial T_a}{\partial \omega_r}=\frac{1}{2\omega_r}\rho A v^3\,\frac{\partial C_p}{\partial \omega_r}-\frac{1}{2\omega_r^2}\rho A v^3\,C_p$$

$$\frac{\partial T_a}{\partial v}=\frac{1}{2\omega_r}\rho A v^3\,\frac{\partial C_p}{\partial v}+\frac{3}{2\omega_r}\rho A v^2\,C_p$$

It is clear from the state space model given in Eq. (7) that the system matrix A and the disturbance matrix E are not fixed matrices and depend on state variables, the uncontrollable input v, and the partial derivatives of the usually non-analytical function of λ and β, C_p. Hence, to cope with system nonlinearity, a nonlinear control strategy is required to achieve the aim and objectives of wind turbine operation.

3-2. The T-S model of the wind turbine

Due to the nonlinear behaviour of the aerodynamic subsystem and its dependence on the wind speed, it is decided to use the T-S fuzzy model based control strategy to design active sensor FTTC. Several reasons lead to satisfaction that a T-S fuzzy nonlinear control can cope with wind turbine control requirements, these are:

- The T-S fuzzy control makes use of a linear control strategy locally to produce a nonlinear controller through fuzzy inference modelling, in terms of fuzzy multiple-modelling.
- By increasing the number of premise variables, the T-S fuzzy model can cover a wider range of operation scenarios which cannot be considered with a linear robust controller. For example, a linear robust controller is designed based on the linearized model derived at a specific operating point belong to the ideal operation curve given in Fig.4. Hence, all other operating regions are considered as modelling uncertainty. Moreover, this controller design always degrades the nominal required performance in order to take good care of the modelling uncertainty. On the other hand, by considering the wind speed and the rotor speed as premise variables in the low wind speed range (*Region2* in Fig. 4), the T-S fuzzy model can approximate the wind turbine model not only during its ideal operation curve but it can additionally cover the operation scenarios in which the system inputs and outputs deviated from ideal operation trajectory. This scenario usually happens during wind turbine operation, specifically for large inertia wind turbines, since the variation of wind speed is faster than rotor speed variations.
- The structure of the nonlinear state space model given in Eq. (7) is characterised by its common input (B) and common output (C) matrices. This fact plays a vital role in simplification and conservatism reduction of T-S fuzzy controller design (Tanaka and Wang, 2001). For example, the quadratic parameterisation of the dynamic output

feedback controller can be reduced to a linear parameterisation dynamic output feedback controller to control the wind turbine.

The aim is to develop a controller whose gain varies with wind speed. For example, in the low wind speed range of operation the control aim is to maximise the amount of power extracted from the available wind power through tracking the optimal rotor rotational speed (ω_{ropt}) reference signal. Hence, to derive the T-S model with minimum uncertainty, the wind speed (v) and the rotor speed (ω_r) are considered as premise variables.

During the low wind speed of operation (*Region 2*) the v varies within the operating range:

$$v \in [v_{min}, v_{max}]\ m\ s^{-1}$$

where in the benchmark wind turbine considered in this paper $v_{min} = 4\ m\ s^{-1}$ and $v_{max} = 12.5\ m\ s^{-1}$. According to these limits the other premise variable (ω_r) is bounded by:

$$\omega_r \in [\omega_{min}, \omega_{max}]\ rad\ s^{-1}$$

where $\omega_{min} = 0.56\ rad\ s^{-1}$ and $\omega_{max} = 1.74\ rad\ s^{-1}$. The bounds of ω_r are determined using Eq. (2) using $\lambda_{opt} = 8$.

The membership function is selected as follows:

$$\left.\begin{aligned} M_1 &= \frac{\omega_r - \omega_{min}}{\omega_{max} - \omega_{min}} \\ M_2 &= 1 - M_1 \\ N_1 &= \frac{v - v_{min}}{v_{max} - v_{min}} \\ N_2 &= 1 - N_1 \end{aligned}\right\} \tag{8}$$

Based on these two premise variables four local linear models of the wind turbine can be determined to approximate the nonlinear system at different operating points in the low range of wind speed. Hence, Eq. (9) gives the four rule T-S fuzzy model of the nonlinear wind turbine in Eq. (7):

$$\left.\begin{aligned} \dot{x} &= \sum_{i=1}^{r} h_i(v, \omega_r)\,[A_i x(t) + Bu + E_i v] \\ y &= Cx(t) \end{aligned}\right\} \tag{9}$$

where $h_1 = M_1 * N_1$, $h_2 = M_1 * N_2$, $h_3 = M_2 * N_1$, and $h_4 = M_2 * N_2$.

Remark 1:

Clearly, more fuzzy rules can approximate nonlinear systems more accurately. However, as the number of fuzzy rules increases, computation burden and design conservatism are unavoidable so that there might be no feasible solution to the set of LMI design constraints. Therefore, the two conditions are partially conflicting with each other, and a trade-off between the number of fuzzy rules and design conservatism should be made.

3-3. Wind turbine control

In order to best understand the wind turbine control challenges, the fundamental theory of the wind power extraction process and the upper bound of conversion efficiency $C_{pmax}(\lambda, \beta)$ of the captured power P_{cap} to the wind power P_{wind} must first be clarified.

Basically, actuator disc theory is used to derive the P_{cap} given in Eq. (1) and the maximum $C_p(\lambda, \beta)$. The actuator disc is a generic device that has the ability to extract wind energy when it is immersed in airflow passing through a virtual tube (see Fig. 2).

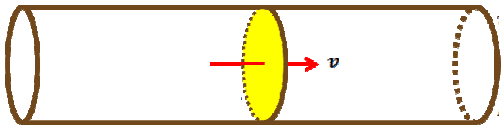

Fig. 2: Actuator disc

the maximum power captured by disc actuator will be (Odgaard, Stoustrup and Kinnaert, 2013):

$$P_{cap} = \frac{1}{2}\rho A v^3 \frac{16}{27} = 0.59 P_{wind} \tag{10}$$

Clearly, the three blade variable speed variable pitch wind turbines are a special case of the actuator disc. In this special structure of actuator disc the blade pitch angles (β), wind speed (v) and the rotor rotational speed (ω_r) are the main variables that affect the amount of the power captured (i.e. C_p). See Fig. 3.

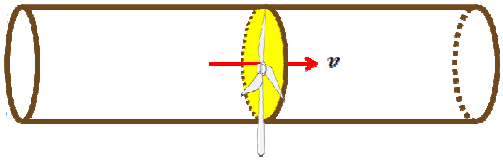

Fig. 3: Wind turbine power extraction

As wind turbines are driven by a naturally generated wind force, the operating range is divided into four regions according to wind speed (See Fig. 4.). *Region 1*, this region is also called the *cut-in* region, in which the wind speed is not sufficient to overcome the wind turbine inertia and hence there is no electrical power generated. *Region 2* in which the wind speed is above the cut-in and below the rated wind speed, the wind turbine objective here is to maximize the amount of the power harvested from the wind and transfer it to electrical power. *Region 3* in which the wind speed is high and rotational speed is equal or above the rated speed and below the *cut-out* speed, the objective is to regulate the generated electrical power to be equal to the rate power. *Region 4* in which the wind speed goes above the upper limit of the predefined working range.

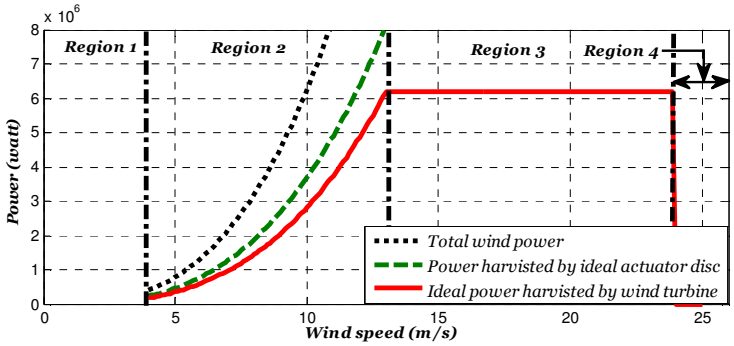

Fig. 4: Wind turbine region of operation.

Fig. 4 shows that wind turbine operation requires different control objective for different ranges of wind speed. Clearly, to achieve wind turbine control objectives, different system variables should be controlled for each specific range of wind speed. The controlled variables could be investigated from the relationship between the power conversion efficiency, the wind speed, and the tip speed ratio as shown in Fig. 5.

Usually, wind speed v and rotor rotational speed ω_r are given in terms of the tip speed ratio λ. The variation of power conversion efficiency with respect to λ and β is given either as a mathematical polynomial or as look-up table. Fig.5 below shows this relationship for the benchmark wind turbine considered in this paper.

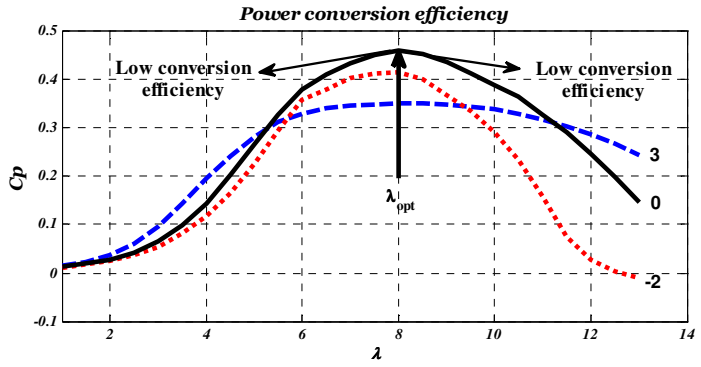

Fig. 5: Variation of C_p with respect to λ at various β

From Fig.5 two points must be highlighted:

1. For low wind speeds, to maximize the amount of the captured wind power the blade pitch angle β must be held at a fixed angle corresponding to maximum allowable conversion efficiency curve at which ($\beta = 0$). Additionally, the rotor speed must vary in proportional to the wind speed variation so that λ is kept in the vicinity of its optimal valueλ_{opt}(i.e. track the optimal rotor rotational speed signal $\omega_{ropt} = \frac{\lambda_{opt} v}{R}$). Specifically, the generator subsystem represents the actuator of the aerodynamic subsystem in the low range of wind speed that decelerates or just releases the aerodynamic subsystem rotation to adjust the variation of rotor speed, so that good tracking of the ω_{ropt} ensured. It should be noted that exact tracking of the ω_{ropt} leads to increasing the load on the drive train shafts and hence minimises the drive train life time. Moreover, exact tracking will also produces a highly fluctuating output power and produce a varying direction reference torque signals that can lead to abnormal generator operation (Munteanu, Bratcu, Cutululis and Ceanga, 2008).
2. For high wind speeds, it is possible to dissipate some proportion of the available wind power by changing the blade pitch angle to prevent the wind turbine operation from crossing over the rated power (i.e. regulate wind turbine operation at the rated power). However, to ensure good regulation performance, some control strategies use the generator torque control as a supplementary control signal to overcome the limited rate of change of blade pitch actuator.

The λ_{opt} is determined by relating the blade time t_b and the turbulence time t_w. t_b is the time required by the blade to take the position of the previous one and t_w is the time required to remove the disturbed wind component generated by the movement of the blade. According to these two times, three operation scenarios can be recognized (Sami, 2012), these are:

a) $t_b > t_w$: This scenario corresponds to slow rotation in which some undisturbed wind passes the area swept by the rotor without harvesting its power content.

b) $t_b < t_w$: This scenario corresponds to fast rotation in which the blade passes through the disturbed wind component generated by the previous blade. In this case the rotor acts as a rigid obstacle and prevents the undisturbed wind from passing through the rotor.

c) $t_b \approx t_w$: This scenario corresponds to the optimal operation in which the blade harvests the power from the re-established wind component.

Hence, wind turbines must be properly controlled to operate in the vicinity of λ_{opt}, at which $t_b \approx t_w$, in order to extract as much wind power as possible.

Remark 2:

- The controller designer must consider several factors that characterise the wind turbine systems such as the requirement of different control objective for different ranges of wind speed, the nonlinearity of the aerodynamic subsystem, the lack of accurate measurement of the wind speed, and the probability of fault occurrence.

- Exact tracking leads to increased loading on the two drive train shafts and hence can shorten the drive train life time. This also produces a highly fluctuating output power, and may even produce a varying direction reference torque signal that can lead to abnormal generator operation. It is thus very clear that the multi-objective approach cannot be avoided for robust wind turbine control design.

4. The active sensor FTTC strategy

This Section focuses on the presentation of a combination of T-S fuzzy PPIO and TSDOFC for wind turbine sensor FTTC based on the scheme shown in Fig. 1. The advantageous features offered by the proposed strategy is that the T-S fuzzy PPIO and the TSDOFC are independently designed, and their performances are considered simultaneously, which is convenient for calculating the design parameters and can avoid the coupling problem generated by the observer-based state feedback control (see remark 3).

Remark 3:

In the fuzzy control design, each "local control" is designed from the corresponding local linear model of a T-S fuzzy model and the fuzzy controller design problem is to determine the local feedback gains within a *parallel distributed compensation* structure (Tanaka and Wang, 2001). Although the fuzzy controller is constructed using the local design structure, the feedback gains should be determined using global design conditions. It is reported in (Tanaka and Wang, 2001) that for the fuzzy state estimate feedback control "*the global design conditions are needed to guarantee the global stability and control performance*". Hence, the fuzzy control designer does not have freedom to assign the local system closed-loop poles anywhere in the stable complex plane. Therefore, the observer-based T-S state feedback control system suffers a major drawback in that the observer dynamics may not be assigned freely to satisfy closed-loop performance requirements (i.e. the separation principle cannot be ensured even when the model uncertainty is not considered). On the other hand, the sensor faults proposed in the benchmark model have an abrupt change behaviour (Odgaard, Stoustrup and Kinnaert, 2013) for which the use of fast fault estimation observer is of great advantage. Hence, the combination of T-S PPIO and TSDOFC is proposed in this strategy to overcome the limitation of T-S observer-based state feedback control.

4-1. The T-S fuzzy PPIO design

Owing to the fact that obtaining accurate fault estimate signals automatically implies FDD, the FDD and FTC literature have shown a constant increase in interest in developing observers that provide estimates of state and fault signals simultaneously. Within this framework, proportional state estimator augmented with integral term (PIO) has been developed as an extension to the well-known Luenberger observer. Specifically, the PIO are observers in which an additional term, proportional to the integral of the output estimation error, is added in order to provide estimates of constant or slowly varying fault signals.

Since, in the fault estimation and compensation based FTC, post-fault system performance is highly affected by the estimation accuracy of the fault signal and, on the other hand, the fault is an unpredictable event in both its occurring time and its behaviour, the fault estimation strategy must have due care for the time varying nature of the fault.

To enhance fault estimate capability of the PIO (i.e. provide accurate estimation for time-varying fault scenarios), T-S fuzzy proportional state estimators augmented with proportional and integral feedback fault estimators (T-S fuzzy PPIO) is presented in this section. The augmented proportional plus integral fault estimator provides degrees of design freedom to shape the estimator tracking performance and hence enhances the FTC loop performance.

Consider the wind turbine system with sensor fault signal as follows:

$$\left.\begin{aligned} \dot{x} &= A(p)x + Bu + E(p)v \\ y &= Cx + D_f f_s \end{aligned}\right\} \tag{11}$$

The system matrices $A(p) \in \mathcal{R}^{n*n}(= \sum_{i=1}^{r} h_i(p)A_i)$, $B \in \mathcal{R}^{n*m}$, $E(p) \in \mathcal{R}^{n*m_v}(= \sum_{i=1}^{r} h_i(p)E_i)$, $D_f \in \mathcal{R}^{l*g}$ and $C \in \mathcal{R}^{l*n}$ are known, r is the number of fuzzy rules, $f_s = [f_{sr} \quad f_{sg}]^T \in \mathcal{R}^g$, and the term $h_i(p)$ is the weighting function satisfying $\sum_{i=1}^{r} h_i(p) = 1$, and $1 \geq h_i(p) \geq 0$, for all t.

Let $e_f \in \mathcal{R}^g$ be the fault estimation error defined as:

$$e_f = f_s - \hat{f}_s \tag{12}$$

To avoid the direct multiplication of the sensor and/or noise by the observer gain, an augmented system state with output filter states is constructed. The filtered output is given as follows:

$$\dot{x}_s = -A_s x_s + A_s C x + A_s D_f f_s \tag{13}$$

where $-A_s \in R^{l*l}$ is a stable matrix. The augmented state system is given as:

$$\left.\begin{aligned} \dot{\bar{x}} &= \bar{A}(p)\bar{x} + \bar{B}u + \bar{E}(p)v + \bar{D}_f f_s \\ \bar{y} &= \bar{C}\,\bar{x} \end{aligned}\right\} \tag{14}$$

$$\bar{A}(p) = \begin{bmatrix} A(p) & 0 \\ A_s C & -A_s \end{bmatrix}, \bar{x} = \begin{bmatrix} x_f \\ x_s \end{bmatrix}, \bar{B} = \begin{bmatrix} B \\ 0 \end{bmatrix}$$

$$\bar{E}(p) = \begin{bmatrix} E(p) \\ 0 \end{bmatrix}, \bar{D}_f = \begin{bmatrix} 0 \\ A_s D_f \end{bmatrix}, \bar{C} = [0 \quad I_l]$$

To deal with time-varying fault scenarios and perform fast fault estimation. A fuzzy fast adaptive fault estimator is designed as an extension to the work of (Zhang, Jiang and Cocquempot, 2008) for linear systems. Hence, The following fuzzy observer is proposed to simultaneously estimate the system states and sensor fault.

$$\left.\begin{aligned} \dot{\hat{\bar{x}}} &= \bar{A}(p)\hat{\bar{x}} + \bar{B}u + \bar{D}_f \hat{f}_s + \bar{E}(p)\tilde{v} + \bar{L}(p)(\bar{C}\bar{x} - \bar{C}\hat{\bar{x}}) \\ \dot{\hat{f}}_s(t) &= F(p)\bar{C}(\dot{e}_x + e_x) \end{aligned}\right\} \tag{15}$$

where $\hat{\bar{x}} \in \mathcal{R}^{n+l}$ is the estimation of the state vector $\bar{x}$, $\tilde{v}$ is anemometer measured wind speed, $\bar{L}(p) \in \mathcal{R}^{(n+l)\times l}$, and $F(p) \in \mathcal{R}^{g\times l}$ are the observer gains to be designed, and e_x is the state estimation error defined as:

$$e_x = \bar{x} - \hat{\bar{x}} \tag{16}$$

The estimator in (15) provides simultaneous estimation of system state and fault signal.

Remark 4:

The observability of (11) implies the observability of the augmented system (15), this can be easily proved from the observability condition:

$$rank\begin{bmatrix} sI - A(p) & 0 \\ A_s C & sI + A_s \\ 0 & I \end{bmatrix} = n + l \quad , \forall s \in \mathbb{C}$$

Also, the rank condition is achieved since $\bar{C}\bar{D}_f = A_s D_f$ and A_s is invertible, then $rank(\bar{C}\bar{D}_f) = rank(A_s D_f) = g$.

The state estimation error dynamic then:

$$\dot{e}_x = (\bar{A}(p) - \bar{L}(p)\bar{C})e_x + \bar{D}_f e_f + \bar{E}(p)e_v \tag{17}$$

e_v is the difference between the effective wind speed and the anemometer measured wind speed. Using (15) and (17) the fault estimation error dynamics are then as follows:

$$\dot{e}_f = \dot{f}_s - F(p)\bar{C}(\bar{A}(p) - \bar{L}(p)\bar{C} + \sigma)e_x - F(p)\bar{C}\bar{D}_f e_f - F(p)\bar{C}\bar{E}(p)e_v \tag{18}$$

The augmented estimator will then be of the following form:

$$\dot{\tilde{e}}_a(t) = \tilde{A}(p,p)\tilde{e}_a + \tilde{N}(p,p)\tilde{z} \tag{19}$$

$$\tilde{A}(p,p) = \begin{bmatrix} \bar{A}(p) - \bar{L}(p)\bar{C} & \bar{D}_f \\ -F(p)\bar{C}(\bar{A}(p) - \bar{L}(p)\bar{C} + I) & -F(p)\bar{C}\bar{D}_f \end{bmatrix}$$

$$\tilde{e}_a = \begin{bmatrix} \mathrm{e_x} \\ e_f \end{bmatrix}, \tilde{z} = \begin{bmatrix} e_v \\ \dot{f}_s \end{bmatrix}, \tilde{N}(p,p) = \begin{bmatrix} \bar{E}(p) & 0 \\ -F(p)\bar{C}\bar{E}(p) & I \end{bmatrix}$$

The objective is to compute the gains $\bar{L}(p)$ and $F(p)$ such that the exogenous input $\tilde{z}$ in (19) are attenuated below the desired level γ to ensure robust regulation performance in addition to locating the observer poles within a specified disc region characterized by its radius (α) and centre (β).

Remark 5:

In the synthesis of control system, some desired performances should be considered in addition to stability. Since classical stability conditions do not deal with transient responses of the closed-loop system, a satisfactory transient response can be guaranteed by confining its poles in a prescribed region. For many real problems, exact pole assignment may not be necessary and it suffices to locate the closed-loop poles in a prescribed subregion in the complex plane. Within this framework (Chilali and Gahinet, 1996) proposed that a convex region in s-plane which represents the desired closed-loop pole-placement constraints can be represented as LMI.

Consequently, in this paper, the transient performance of the nonlinear system represented by T-S model is governed by applying the Chilali and Gahinet's LMI regions to each local T-S fuzzy controller. Hence, for each local pair of $A(p)$ and C matrices there will be observer gain $L(p)$ (obtained offline during the design stage) that satisfies the feasibility of global stability as well as pole-placement LMIs.

Theorem 1. The estimation error system eigenvalues are located in a disc region in the complex plane defined by (α, β) so that the error dynamics are stable. Furthermore, the H_∞ performance is guaranteed with an attenuation level γ, (provided that the signal $(\dot{f}_s)$ is bounded), if there exist symmetric positive definite matrix P_1, matrices H_i, F_i, and a scalar μ, α, and β satisfying the following LMI constraints:

$$\begin{bmatrix} -\alpha P_1 & 0 & \phi_1 & \phi_2 \\ 0 & -\alpha I & \phi_3 & \phi_4 \\ * & * & -\alpha P_1 & 0 \\ * & * & 0 & -\alpha I \end{bmatrix} < 0 \tag{20}$$

$$\begin{bmatrix} \Psi_{11} & \Psi_{12} & \Psi_{13} & 0 & C_{p1}^T & 0 \\ * & \Psi_{22} & \Psi_{23} & I & 0 & C_{p2}^T \\ * & * & -\gamma I & 0 & 0 & 0 \\ * & * & * & -\gamma I & 0 & 0 \\ * & * & * & * & -\gamma I & 0 \\ * & * & * & * & * & -\gamma I \end{bmatrix} < 0 \tag{21}$$

$\bar{L}(p) = P_1^{-1}\bar{H}(p)$, $\Psi_{11} = P_1\bar{A}(p) + \left(P_1\bar{A}(p)\right)^T - \bar{H}(p)\bar{C} - (\bar{H}(p)\bar{C})^T$, $\Psi_{12} = -(\bar{A}^T(p)P_1\bar{D}_f - \bar{C}^T\bar{H}^T(p)\bar{D}_f)$

$\Psi_{13} = P_1\bar{E}(p)$, $\Psi_{22} = -_2\bar{D}_f{}^T P_1\bar{D}_f$, $\Psi_{23} = -\bar{D}_f{}^T P_1\bar{E}(p)$

$\phi_1 = P_1\bar{A}(p) - \bar{H}(p)\bar{C} + \beta P_1$, $\phi_2 = P_1\bar{D}_f$,

$\phi_3 = -\left(\bar{A}^T(p)P_1\bar{D}_f - \bar{C}^T\bar{H}^T(p)\bar{D}_f + \bar{D}_f{}^T P_1\right)^T$

$\phi_4 = -\bar{D}_f{}^T P_1\bar{D}_f + \beta I$

Proof. Let the performance output be defined as follows:

$\tilde{e}_p = \bar{C}_p\,\tilde{e}_a$, $\bar{C}_p = \begin{bmatrix} C_{p1} & 0 \\ 0 & C_{p2} \end{bmatrix}$

$C_{p1} \in \mathcal{R}^{k*n}$ and $C_{p2} \in \mathcal{R}^{g*g}$. The estimation performance objective can be presented mathematically as follows:

$$\frac{\|\tilde{e}_p\|_2}{\|\tilde{z}\|_2} \le \gamma = \frac{1}{\gamma}\int_0^\infty \tilde{e}_a^T\,\bar{C}_p^T\bar{C}_p\tilde{e}_a dt - \gamma\int_0^\infty \tilde{z}^T\,\tilde{z} \le 0 \tag{22}$$

Consider the following candidate Lyapunov function for the augmented system

$$v(\tilde{e}_a) = \tilde{e}_a^T\,\bar{P}\,\tilde{e}_a \;, where\ \bar{P} > 0 \tag{23}$$

To achieve the required performance (22) and the stability of the augmented system the following inequality should hold:

$$\dot{v}(\tilde{e}_a) + \frac{1}{\gamma}\tilde{e}_p^T\,\tilde{e}_p - \gamma\tilde{z}^T\tilde{z} < 0 \tag{24}$$

where $\dot{v}(\tilde{e}_a)$ is the derivative of candidate Lyapunov function in terms of , it will become:

$$\dot{v}(\tilde{e}_a) = \tilde{e}_a^T\left(\tilde{A}^T(p,p)\bar{P} + \bar{P}\tilde{A}(p,p)\right)\tilde{e}_a + \tilde{e}_a^T\bar{P}\tilde{N}(p,p)\tilde{z} + \tilde{z}^T\tilde{N}^T(p,p)\bar{P}\tilde{e}_a \tag{25}$$

By using (25), and the Schur Complement theorem, inequality (24) implies that the following inequality holds:

$$\begin{bmatrix} \tilde{A}^T(p,p)\bar{P} + \bar{P}\tilde{A}(p,p) & \bar{P}\tilde{N}(p,p) & \bar{C}_{p1}^T & 0 \\ * & -\gamma I & 0 & \bar{C}_{p2}^T \\ * & * & -\gamma I & 0 \\ * & * & * & -\gamma I \end{bmatrix} < 0 \tag{26}$$

To conform to the format of $\bar{P}$ is structured as follows:

$$\bar{P} = \begin{bmatrix} P_1 & 0 \\ 0 & I \end{bmatrix} > 0 \tag{27}$$

Substituting the corresponding values of$\bar{P}, \tilde{A}(p,p), \tilde{N}(p,p)$ and using the variable change $\bar{H}(p) = P_1\bar{L}(p)$, and equality

$$F(p)\bar{C} = \bar{D}_f{}^T P_1 \tag{28}$$

the LMI in (21) is thus obtained.

To prove LMI (20) we first need the following Lemma from (Chilali and Gahinet, 1996, Mansouri, Manamanni, Guelton and Djemai, 2008).

Lemma1: The matrix *A* is D-stable if and only if there exists a symmetric matrix *X* such that:

$$\begin{bmatrix} -\alpha X & \beta X + XA \\ \beta X + (XA)^T & -\alpha X \end{bmatrix} < 0\,, \qquad X > 0 \tag{29}$$

Based on Lemma 1 one can obtain inequality (20) after substituting:

$X = \bar{P} = \begin{bmatrix} P_1 & 0 \\ 0 & I \end{bmatrix} > 0$, $A = \tilde{A}(p,p)$ defined in (24).

This completes the proof of Theorem 1.

4-2. The TSDOFC design

The control objective here is to design a dynamic output feedback controller capable of forcing the generator rotational speed of the wind turbine to follow the optimal generator speed signal in both faulty and fault-free cases.

An augmented system consisting of the system (11) and the integral of the tracking error $e_{ti} = \int(y_r - Sy)$ is defined as:

$$\left.\begin{aligned} \dot{\bar{x}} &= \bar{A}(p)\bar{x} + \bar{B}u + \bar{E}(p)\delta + Ry_r + D_{in}e_f \\ \bar{y} &= \bar{C}\,\bar{x} + \bar{D}_f e_f \end{aligned}\right\} \tag{30}$$

$$\bar{A}(p) = \begin{bmatrix} 0 & -SC \\ 0 & A(p) \end{bmatrix}, \bar{x} = \begin{bmatrix} e_{ti} \\ x \end{bmatrix}, \bar{B} = \begin{bmatrix} 0 \\ B \end{bmatrix}$$

$$D_{in} = \begin{bmatrix} -SD_f \\ 0 \end{bmatrix}, \bar{E}(p) = \begin{bmatrix} 0 \\ E(p) \end{bmatrix}, R = \begin{bmatrix} I \\ 0 \end{bmatrix}$$

$$\bar{C} = \begin{bmatrix} I & 0 \\ 0 & C \end{bmatrix}, \bar{D}_f = \begin{bmatrix} 0 \\ D_f \end{bmatrix}$$

where $S \in \mathcal{R}^{q*l}$ is used to define which output variable is considered to track the reference signal. Since the system in (11) has common input and output matrices (*B* & *C*), the dynamic output feedback controller used to stabilize and perform the tracking objective is of linear parameterisation form and defined as:

$$\left.\begin{aligned}\dot{x}_c &= A_c(p)x_c + B_c(p)(S_r y_r - \bar{y}) \\ u &= C_c(p)x_c + D_c(p)(S_r y_r - \bar{y})\end{aligned}\right\} \tag{31}$$

where x_c is the state and $A_c(p) \in \mathcal{R}^{(n+q)\times(n+q)}$, $B_c(p) \in \mathcal{R}^{(n+q)\times(l+q)}$, $C_c(p) \in \mathcal{R}^{m\times(n+q)}$, $D_c \in \mathcal{R}^{m\times(l+q)} and\ S_r \in \mathcal{R}^{(l+q)\times q}$ is introduced to match the dimensions of $y_r\ and\ \bar{y}$.

Remark 6:

In general, the TSDOFC can have cubic, quadratic, or linear parameterisation. For a given T-S model, the choice of particular TSDOFC parameterisation is influenced by the structure of the T-S subsystems. While cubic parameterisation is required for parameter dependent $A, B,$ and C matrices T-S fuzzy model, the linear parameterisation fuzzy controller is suitable for common input and common output matrices.

Aggregation of (30) and (31) gives the following system:

$$\left.\begin{aligned}\dot{x}_a &= A_a(p)x_a + E_a(p)d \\ \bar{y} &= C_a x_a + D_a d\end{aligned}\right\} \tag{32}$$

$$A_a(p) = \begin{bmatrix}\bar{A}(p) - \bar{B}D_c(p)\bar{C} & \bar{B}C_c(p) \\ -B_c(p)\bar{C} & A_c(p)\end{bmatrix}, d = \begin{bmatrix}\delta \\ e_f \\ y_r\end{bmatrix}$$

$$x_a = \begin{bmatrix}\bar{x} \\ x_c\end{bmatrix}, C_a = [\bar{C} \quad 0], D_a = \begin{bmatrix}0 & \bar{D}_f & 0\end{bmatrix}$$

$$E_a(p) = \begin{bmatrix}\bar{E}(p) & D_{in} - \bar{B}D_c(p)\bar{D}_f & R + \bar{B}D_c(p)S_r \\ 0 & -B_c(p)\bar{D}_f & B_c(p)S_r\end{bmatrix}$$

Theorem 2. The eigenvalues of the closed-loop system (32) are located in the disc region of the negative complex plane characterised by radius (α), centre (β), and the closed-loop is stable and tracks the reference signal with guaranteed H_∞ performance and with an attenuation level γ, (provided that the signals in d are bounded), if there exist symmetric positive definite matrices X, Y and matrices $A_c(p)$,$B_c(p)$,$C_c(p)$, and $D_c(p)$ satisfying the following LMI constraints:

$$\begin{bmatrix}-\alpha X & -I & \phi_{1c} & \phi_{2c} \\ -I & -\alpha Y & \phi_{3c} & \phi_{4c} \\ * & * & -\alpha X & 0 \\ * & * & 0 & -\alpha Y\end{bmatrix} < 0 \tag{33}$$

$$\begin{bmatrix}\Psi_{11c} & \Psi_{12c} & \bar{E}(p) & \Psi_{13c} & \Psi_{14c} & XC_{p1}^T \\ * & \Psi_{22c} & Y\bar{E}(p) & \Psi_{23c} & \Psi_{24c} & C_{p1}^T \\ * & * & -\gamma I & 0 & 0 & 0 \\ * & * & * & -\gamma I & 0 & 0 \\ * & * & * & * & -\gamma I & 0 \\ * & * & * & * & * & -\gamma I\end{bmatrix} < 0 \tag{34}$$

where

$$\Psi_{11c} = \bar{A}(p)X + (\bar{A}(p)X)^T + \bar{B}\hat{C}(p) + \left(\bar{B}\hat{C}(p)\right)^T$$

$$\Psi_{12c} = \hat{A}^T(p) + \bar{A}(p) - \bar{B}\hat{D}(p)\bar{C}$$

$$\Psi_{13c} = D_{in} - \bar{B}(p)\hat{D}(p)\bar{D}_f$$

$$\Psi_{22c} = Y\bar{A}(p) + \left(Y\bar{A}(p)\right)^T + \hat{B}(p)\bar{C} + \left(\hat{B}(p)\bar{C}\right)^T$$

$$\Psi_{23c} = YD_{in} + \hat{B}(p)\bar{D}_f$$

$$\Psi_{14c} = R + \bar{B}\hat{D}(p)S_r\ ;\ \Psi_{24c} = YR - \hat{B}(p)S_r$$

$$\phi_{1c} = \bar{A}(p)X + \bar{B}\hat{C}(p) + \beta X\ ;\ \phi_{2c} = \bar{A}(p) - \bar{B}\hat{D}(p)\bar{C} + \beta I$$

$$\phi_{3c} = \hat{A}(p) + \beta I\ ;\ \phi_{4c} = Y\bar{A}(p) + \hat{B}(p)\bar{C}(p) + \beta Y$$

The controller gains are thus calculated as follows:

$D_c(p) = \widehat{D}(p)$

$C_c(p) = \left(\hat{C}(p) + D_c(p)\bar{C}X\right)M^{-T}$

$B_c(p) = N^{-1}(-\hat{B}(p) - Y\bar{B}D_c(p)$

$A_c(p) = N^{-1}(\hat{A}(p) - Y\left(\bar{A}(p) - \bar{B}\widehat{D}(p)\bar{C}\right)X - Y\bar{B}C_c(p)M^T + NB_c(p)\bar{C}X)M^{-T}$

where $M\ and\ N$ satisfy $MN^T = I - XY$

Proof. Let the output performance y_p be defined as:

$y_p = \bar{C}_p\ \bar{y}$

Where $\bar{C}_p$ is selected according to design requirements. The objective of the controller design performance can presented mathematically as:

$$\frac{\|y_p\|_2}{\|d\|_2} \leq \gamma = \frac{1}{\gamma}\int_0^\infty \bar{y}^T\ \bar{C}_p^T\bar{C}_p\bar{y}dt - \gamma\int_0^\infty d^T\ d\ \leq 0 \tag{35}$$

Consider the following candidate Lyapunov function for the augmented system (32):

$v(x_a) = x_a^T\ \bar{P}_c\ x_a\ \ ,where\ \bar{P}_c > 0$

To achieve the required performance (35) and stability of the augmented system (32) the following inequality should hold:

$$\dot{v}(x_a) + \frac{1}{\gamma}y_p^T\ y_p - \gamma d^T d < 0 \tag{36}$$

where $\dot{v}(x_a)$ is the derivative of candidate Lyapunov function. In terms of (32), this becomes:

$$\dot{v}(x_a) = x_a^T\left(A_a^T(p)\bar{P}_c\ + \bar{P}_cA_a(p)\right)x_a\ +\ x_a^T\bar{P}_cE_a(p)d + d^TE_a^T(p)\bar{P}_cx_a \tag{37}$$

By using (37), and the Schur Complement Theorem, inequality (36) implies that the following inequality must hold:

$$\begin{bmatrix} A_a^T(p)\bar{P}_c\ + \bar{P}_cA_a(p) & \bar{P}_cE_a(p) & \bar{C}_p^T \\ * & -\gamma I & 0 \\ * & * & -\gamma I \end{bmatrix} < 0 \tag{38}$$

assume $\bar{P}_c$ and $\bar{P}_c^{-1}$ is structured as $\bar{P}_c = \begin{bmatrix} Y & N \\ N^T & W \end{bmatrix}$, $\bar{P}_c^{-1} = \begin{bmatrix} X & M \\ M^T & Z \end{bmatrix}$

since $\bar{P}_c^{-1}\bar{P}_c = I$ (i.e. $\begin{bmatrix} X & M \\ M^T & Z \end{bmatrix}\begin{bmatrix} Y & N \\ N^T & W \end{bmatrix} = \begin{bmatrix} XY + MN^T & XN + MW \\ M^TY + ZN^T & M^TN + ZW \end{bmatrix} = \begin{bmatrix} I & 0 \\ 0 & I \end{bmatrix}$)

we have $\bar{P}_c\begin{bmatrix} X \\ M^T \end{bmatrix} = \begin{bmatrix} I \\ 0 \end{bmatrix} \Rightarrow \bar{P}_c\begin{bmatrix} X & I \\ M^T & 0 \end{bmatrix} = \begin{bmatrix} I & Y \\ 0 & N^T \end{bmatrix}$.

define $\Pi_1 = \begin{bmatrix} X & I \\ M^T & 0 \end{bmatrix}$; $\Pi_2 = \begin{bmatrix} I & Y \\ 0 & N^T \end{bmatrix}$

Pre and post multiply inequality (38) by diagonals $[\Pi_1^T \quad I \quad I]$ and its transpose and by using the variable change:

$\hat{A}(p) = Y\left(\bar{A}(p) - \bar{B}\widehat{D}(p)\bar{C}\right)X + Y\bar{B}C_c(p)M^T - NB_c(p)\bar{C}X + NA_c(p)M^T$

$\hat{B}(p) = -NB_c(p) - Y\bar{B}D_c(p))$

$\hat{C}(p) = C_c(p)M^T - D_c(p)\bar{C}X$

$\widehat{D}(p) = D_c(p)$

Inequality (34) can thus be easily obtained.

By using Eq. (29) of Lemma1 and the variable change $A = A_a(p), X = \bar{P}_c$ and then by pre- and post-multiplying by diagonal $[\Pi_1^T \quad \Pi_1^T]$ and its transpose respectively, the inequality (33) can be easily obtained.

Remark 7:

- The equality (28) can be relaxed using the following optimization problem (Zhang, Jiang and Cocquempot, 2008).

Minimise μ

$$\begin{bmatrix} \mu I & \bar{D}_f{}^T P_1 - F(p)\bar{C} \\ * & \mu I \end{bmatrix} > 0 \tag{39}$$

- Matrices M, N^T can be calculated based on equality $MN^T = I - XY$ using any matrix decomposition techniques such as ***qr*** or ***svd***.
- Practically, the measured wind speed signal does not exactly represent the effective wind speed signal. However, the proposed strategy makes use of measured wind speed in order to cope with the tradeoff between design complexity and wind speed signal accuracy. However, the fault estimator is designed to be robust against the expected error between the measured and the effective rotor wind speed.
- Due to the large wind turbine inertia, in the practical situation the tracking follows the trends of the speed variation and not the detailed variations.

5. Simulation results

The FTTC system design and simulation results are based on the wind turbine benchmark system proposed by kk-electronic (Odgaard, Stoustrup and Kinnaert, 2009, Odgaard, Stoustrup and Kinnaert, 2013). As illustrated in Section 2, the T-S fuzzy model describing the low wind speed dynamics of the wind turbine is derived depending on two scheduling variables, namely the measured rotor angular velocity ω_r and the wind speed v. The nonlinear system behaviour is approximated using four local linear systems derived to represent the system dynamics at four operating points.

As stated in Section 3-3, the controller optimises the power captured by controlling the rotor rotational speed by varying the reference generator torque T_{gr} so that the wind turbine rotor speed ω_r follows the optimal rotor speed given by:

$$\omega_{ropt} = \frac{\lambda_{opt} v}{R} \tag{40}$$

where ω_{ropt} and λ_{opt} are the optimal rotor speed and the optimal tip speed ratio. In fact, designing a controller for the power optimization problem must achieve the design constraints listed in Remark 2. One of these constraints is to have the capability to tolerate the effects of faults that affect different system components.

The following faults are considered and the proposed control strategies need to tolerate the fault effects so that good tracking performance to ω_{ropt} can be maintained.

Remark 8:

The expected effects of different fault scenarios proposed in the considered benchmark is investigated as follows:

- Scaling measurement sensor fault: this fault scenario represents a loss of effectiveness of the sensor so that the faulty measurement becomes $\omega_{r\,measured} = \alpha\, \omega_{r\,actual}$. Since the tracking problem becomes a regulation problem in terms of the tracking error (e_t). Suppose, following a transient time, that the tracking error (e_t) becomes $(e_t = \omega_{ropt} - \omega_{r\,measured} = 0)$, this implies that: $\omega_{r\,actual} = \omega_{r\,measured}/\alpha$. Hence, from a control stand point, for the case of a sensor fault the controller starts to produce a control signal that minimizes the difference between the faulty measurement and the desired optimal rotor speed. Moreover, as the severity of the sensor fault increases the tracking performance then deeply degrades.
- Stuck measurement sensor fault: $(\omega_{r\,measured} = constant)$ This fault scenario represents the worst sensor fault case since the controller receives measurements that are completely independent of the system states. In fact, this fault leads the controller to generate control signal that forces the closed-loop system to operate away from nominal operating region boundary since whatever control signal is delivered, the measurements are fixed at $C_i x(t) = constant$ and hence $(e_t = \omega_{ropt} - \omega_{r\,measured} \neq 0)$.

- Without loss of generality, the output matrix parametric fault presented in wind turbine benchmark model can be represented as an additive fault in which the fault signal depends on the measured state, as illustrated below:

  Suppose the fault free output is given as:

  $$y = Cx = \begin{bmatrix} 1 & 0 \\ 0 & 1 \end{bmatrix} \begin{bmatrix} x_1 \\ x_2 \end{bmatrix}$$

  Then the parametric sensor fault can be modelled as follows:

  $$y_f = C_f x = \begin{bmatrix} 1 & 0 \\ 0 & 0.9 \end{bmatrix} \begin{bmatrix} x_1 \\ x_2 \end{bmatrix} = Cx + \begin{bmatrix} 0 \\ 1 \end{bmatrix} (-0.1 * x_2) \quad (41)$$

Three fault scenarios are considered in this Section, these are:

1. Generator rotational speed scaling fault (f_{sg}):

The two fault scenarios are 0.9 and 1.1 scale measurements (output matrix parametric changes) of generator rotational speed sensor. As stated in remark8, parameter changes in the output matrix C can be considered as a special case of additive faults in which the fault signals (f_{sg}) is a scaled version of the measured state. Fig.6 shows the two fault scenarios and the effectiveness of the proposed strategy to compensate the bias from the scaled measurements.

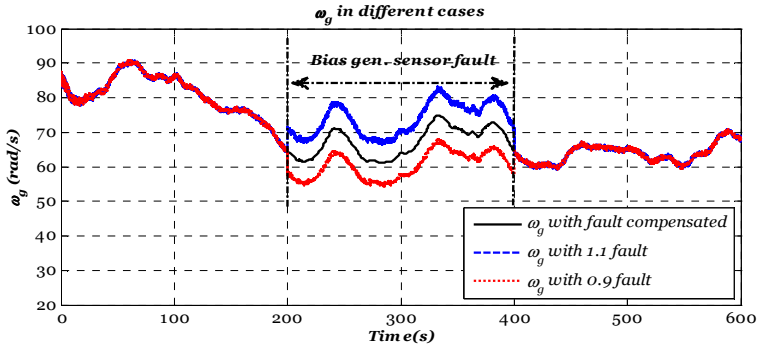

Fig. 6: Effectiveness of compensation strategy .

The ability of the proposed T-S fuzzy PPIO to accurately estimate abruptly changing fault is clearly shown in Fig. 7 (a&b).

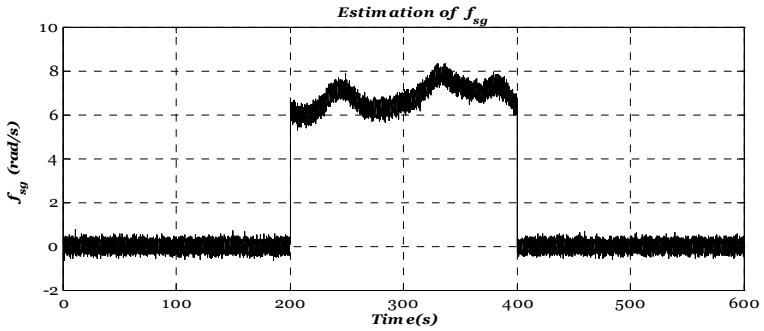

(a)

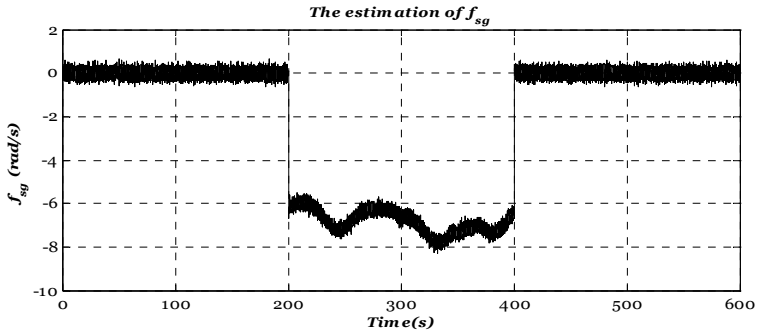

(b)

Fig. 7: Generator rotational speed scale sensor faults estimation (a & b)

The T-S PPIO can provide information about the fault severity via the fault estimation signal. This is achieved through taking the ratio between the measured generator speed $\omega_g$and the estimated signal $\hat{\omega}_g$. Hence, if there are no faults the ratio should be 1 otherwise, any deviation from unity indicates the occurrence of the fault and the magnitude of the deviation represents the fault severity. Fig. 8 shows the fault evaluation signal for both 1.1 ω_g and 0.9 ω_g fault scenarios.

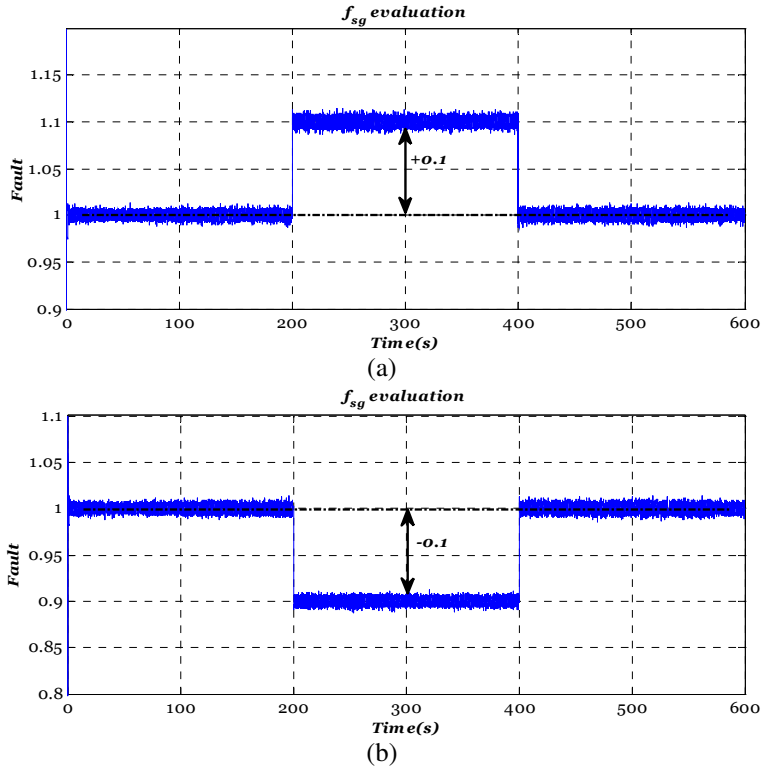

Fig. 8: Deviation of 1.1 (a) and 0.9 (b) sensor measurements from unity

Clearly, the two fault scenarios (1.1 or 0.9 scale fault) affect the wind turbine closed-loop performance and hence the wind power conversion efficiency. However, the expected effect of this fault is probably less than the effect of rotor speed sensor fault since the generator speed signal is part of the feedback signals and not compared directly with the reference optimal speed (i.e. not the objective signal). Fig. 9 shows the tracking of the objective variable ω_r with(out) 1.1 ω_g scaling fault.

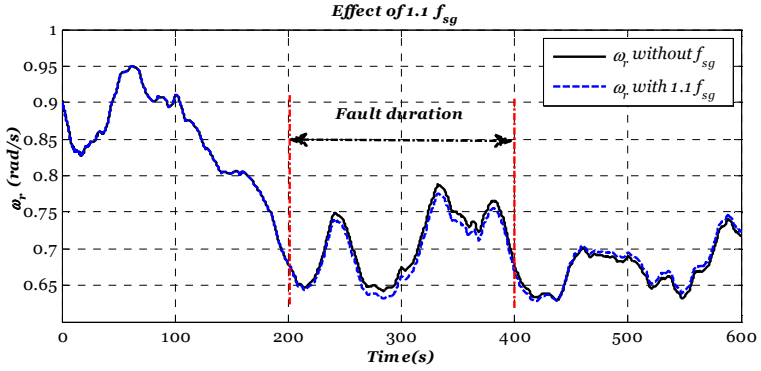

Fig. 9: The effect of generator speed scale sensor fault

Although the $\omega_g$sensor fault has minor effect on the overall closed-loop system performance, the proposed strategy compensates the effect of this fault scenario so that the TSDOFC always receives fault free ω_g measurement.

Remark 9:

As presented in Section 2, the proposed FTTC is based on the estimation and compensation approach to FTC. Within this framework the estimator hides the effect of sensor faults so that the controller always receives a fault-free measurement. Hence, the ability of the proposed FTTC to tolerate bigger fault magnitudes is governed by the ability of T-S fuzzy PPIO

to provide a fault estimation signal. This in turn depends on whether the post fault pairs $(A(p), C)$ satisfy the observability condition (or at least the detectability condition). Fig. 10a shows the generator rotational speed with 1.5 $\omega_g$scale fault. Although this fault has bigger magnitude than 1.1 ω_g, the T-S fuzzy PPIO can provide an accurate fault estimate (see Fig. 10b) which in turn used to compensate (*hide*) the effect of 1.5 ω_g sensor fault from the input of TSDOFC. This is clearly shown in Fig. 10a in which the measured ω_g after fault compensation exactly match the nominal (*fault free*) ω_g.

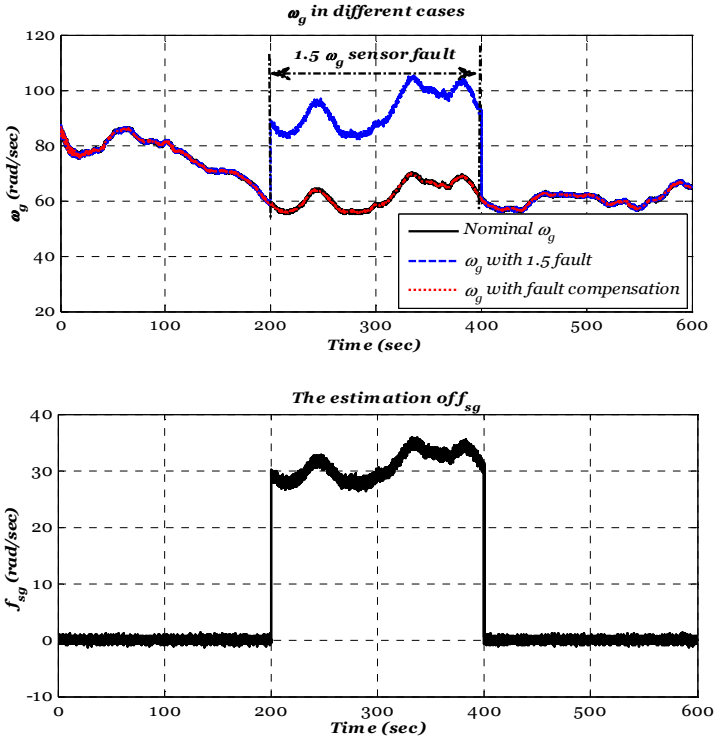

Fig.10: Effectiveness of compensation strategy with 50% scale fault

(a) ω_g in different cases, (b) fault estimation.

2. Rotor rotational speed stuck sensor fault (f_{sr}) $(\omega_{ropt} < \omega_{r\ measured})$

The second fault is represented by the fixed sensor output of the rotor speed sensor at 1.4 $rad\ sec^{-1}$. This fault scenario and the effectiveness of the estimation and compensation strategy to maintain the required system performance in the presence of this fault is shown in Fig. 11.

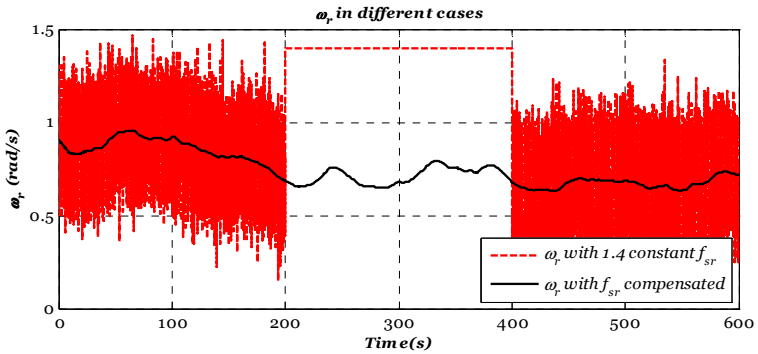

(a)

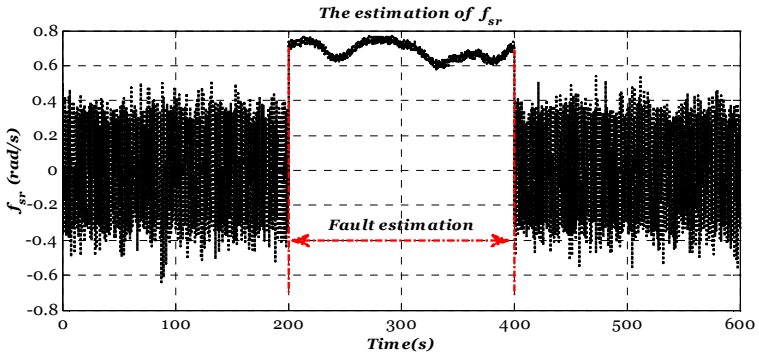

(b)

Fig. 11: The effectiveness of the proposed strategy to tolerate stuck rotor speed sensor fault (a) and fault estimation (b).

The effect of this fault scenario varies according to the fixed measurement of rotor speed and ω_{ropt} which in turn depends on the wind speed. In this case ω_{ropt} is lower than the fixed rotor speed measurement and hence the controller starts to force the system to slow-down the rotor speed (Fig. 12a). Hence, as long as the optimal speed remains below the measured value, the controller keeps increasing the reference generator torque T_{gr} (Fig. 12b) which may lead to the rotaion speed ω_r reaching its cut-off value, i.e. the turbine is shut down due to a rotor rotation speed sensor fault. A further investigation of the effect of stuck sensor fault scenario is shown in Fig. 12. It is clearly shown that this fault scenario can lead to wind turbine shut-down by increasing the breaking action which in turn increases the drive train torsional load.

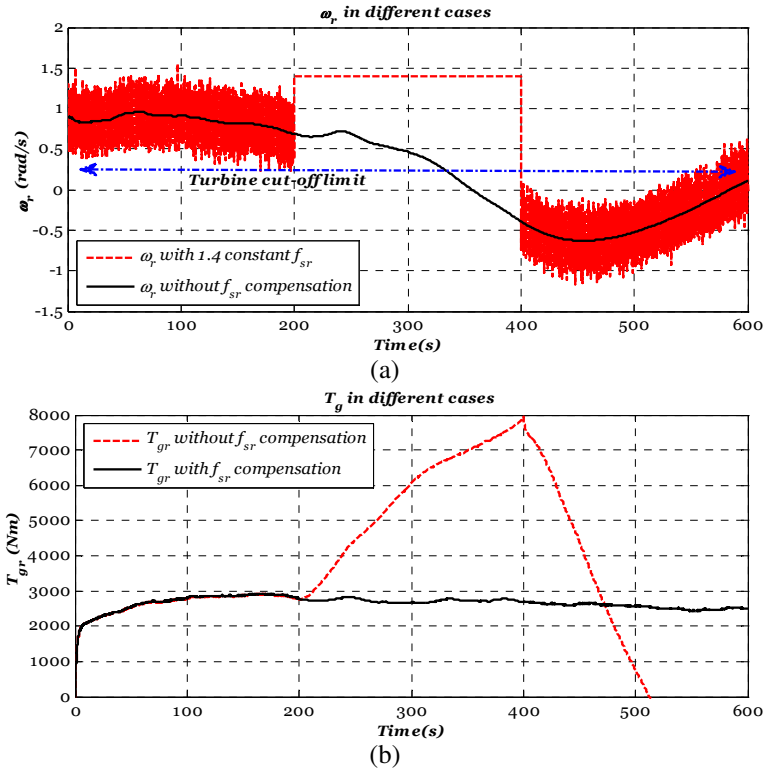

(a)

(b)

Fig. 12: Further investigation of stuck fault effect and the effectiveness of the proposed strategy. (a) Rotor speed and (b) generator torque

3. Rotor rotational speed stuck sensor fault ($\omega_{ropt} > \omega_{r\,measured}$)

In this rotor speed stuck sensor fault scenario ω_{ropt} is higher than the stuck measurement (at $0.5\ rad\ sec^{-1}$) of the rotor speed. The effectiveness of the proposed strategy to tolerate this fault scenario is shown in Fig. 13 (a & b). In this case, the controller will generate a reference generator torque signal (T_{gr}) that simply release the turbine to rotate according to the available wind speed without control (Fig. 13b).

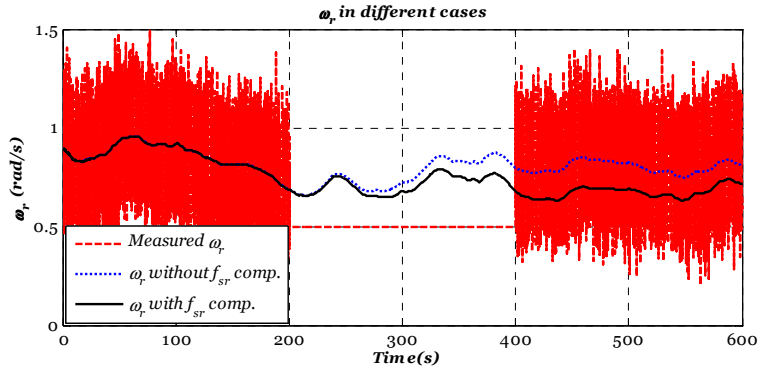

(a)

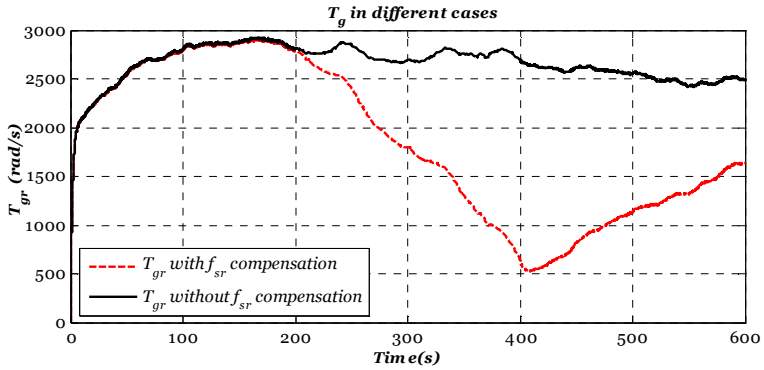

(b)

Fig. 13: The effectiveness of the proposed strategy to tolerate stuck rotor speed sensor fault. (a) Rotor speed and (b) generator torque

On the other hand, Fig. 14 shows the effect of stuck fault scenarios from power capture stand point. For $1.4\,rad\,sec^{-1}$ stuck sensor fault the controller will produce T_{gr} that forces the wind turbine to slow down the actual rotor rotational speed and hence minimises the power capture (Fig. 14 dotted line). On the other hand, $0.5\,rad\,sec^{-1}$ stuck fault will will make the controller produces T_{gr} that simply releas the wind turbine to rotat according to the available wind speed. This in turn will forces the system to operate away from its optimal tip speed ratio (Fig. 14 dashed-dotted line).

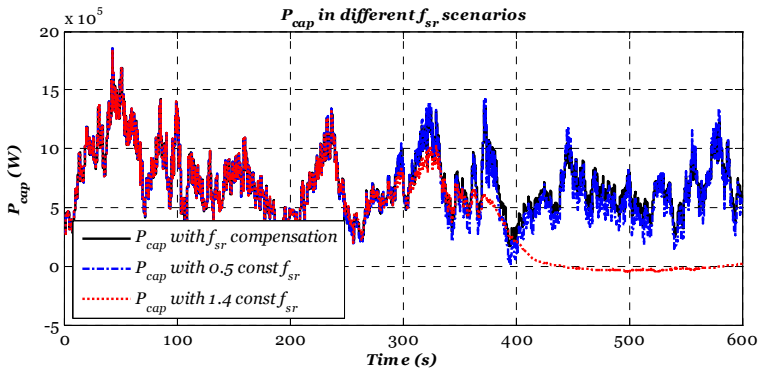

Fig. 14: The effect of stuck fault scenarios on the power captured

4. Conclusion

The paper develops a new architecture for active sensor FTTC for OWT based on fault estimation and compensation. Using this proposed architecture, a detailed design approach is presented for an OWT. A dynamic output feedback control scheme is used that has time-varying reference tracking capability and the fault estimator is designed using a proposed T-S extension of a well known PPI observer scheme, the T-S PPIO. The controller and fault estimator

individually satisfy an appropriate L_2 norm robustness condition guaranteeing minimum tracking error and robust fault estimation. Results are presented illustrating the robustness of the proposed FTTC design using the Safeprocess wind turbine benchmark system.

In summary, wind turbines are nonlinear systems that are driven by a stochastic wind force signal. Sustainability of such systems is highly affected by the chosen control strategy. Several design constraints must be taken into account in the design of the wind turbine power maximization controller, these are:

a. Wind turbines are characterised by their non-linear aerodynamics and have a stochastic and uncontrollable driving force as input in the form of wind speed. This limits the ability of linear control strategies to maintain acceptable performance over a wide range of wind speed.

b. Due to the common input common output matrices of wind turbine model the conservatism of T-S fuzzy estimation and control is highly reduced.

c. Owing to the direct effect of wind turbine components faults on the wind power conversion efficiency, the designed control strategy must be capable of tolerating different expected fault effects.

d. Exact tracking leads to increased loading on the two drive train shafts and hence can shorten the drive train life time. This also produces a highly fluctuating output power, and may even produce a varying direction reference torque signal that can lead to abnormal generator operation. It is thus very clear that the multi-objective approach cannot be avoided for robust wind turbine control design.

e. Due to the stochastic nature of the operating environment and missing or inaccurate wind speed measurements, the wind turbine fault estimation and compensation problem is challenged by a requirement for a robust against the difference between the measured and the actual wind speed.

REFERENCES

Amirat, Y., Benbouzid, M. E. H., Al-Ahmar, E., Bensaker, B. & Turri, S. 2009. A brief status on condition monitoring and fault diagnosis in wind energy conversion systems. *Renewable and Sustainable Energy Reviews,* 13, 9, 2629-2636.

Badihi, H., Zhang, Y. & Hong, H. 2013. Fuzzy gain-scheduled active fault-tolerant control of a wind turbine. *Journal of the Franklin Institute*, http://dx.doi.org/10.1016/j.jfranklin.2013.05.007.

Bianchi, D. F., De Battista, H. & Mantz, J. R. 2007. *Wind Turbine Control Systems: Principles, Modelling and Gain Scheduling Design*, Springer-Verlag.

Chilali, M. & Gahinet, P. 1996. H∞ design with pole placement constraints: an LMI approach. *IEEE Trans. on Automatic Control,* 41, 3, 358-367.

Djurovic, S., Crabtree, C. J., Tavner, P. J. & Smith, A. C. 2012. Condition monitoring of wind turbine induction generators with rotor electrical asymmetry. *Renewable Power Generation, IET,* 6, 4, 207-216.

Hameed, Z., Hong, Y. S., Cho, Y. M., Ahn, S. H. & Song, C. K. 2009. Condition monitoring and fault detection of wind turbines and related algorithms: A review. *Renewable and Sustainable Energy Reviews,* 13, 1, 1-39.

Jain, T., Yame, J. J. & Sauter, D. 2013. A Novel Approach to Real-Time Fault Accommodation in NREL's 5-MW Wind Turbine Systems. *IEEE Trans. on Sustainable Energy,* 4, 4, 1082-1090.

Johnson, K. E. & Fleming, P. A. 2011. Development, implementation, and testing of fault detection strategies on the National Wind Technology Center's controls advanced research turbines. *Mechatronics,* 21, 4, 728-736.

Kamal, E., Aitouche, A., Ghorbani, R. & Bayart, M. 2012. Robust Fuzzy Fault-Tolerant Control of Wind Energy Conversion Systems Subject to Sensor Faults. *IEEE Trans. on Sustainable Energy,* 3, 2, 231-241.

Mansouri, B., Manamanni, N., Guelton, K. & Djemai, M. 2008. Robust pole placement controller design in LMI region for uncertain and disturbed switched systems. *Nonlinear Analysis: Hybrid Systems,* 2, 4, 1136-1143.

Marden, J. R., Ruben, S. D. & Pao, L. Y. 2013. A Model-Free Approach to Wind Farm Control Using Game Theoretic Methods. *IEEE Trans. on Control Systems Technology,* 21, 4, 1207-1214.

Munteanu, I., Bratcu, A., Cutululis, N.-A. & Ceanga, E. 2008. *Optimal Control of Wind Energy Systems: Towards a Global Approach* Springer-Verlag.

Niemann, H. & Stoustrup, J. 2005. Passive fault tolerant control of a double inverted pendulum—a case study. *Control Engineering Practice,* 13, 8, 1047-1059.

Odgaard, P. F., Stoustrup, J. & Kinnaert, M. 2009. Fault Tolerant Control of Wind Turbines: a Benchmark Model. 7th IFAC Symposium on Fault Detection, Supervision and Safety of Technical Processes *Safeprocess 2009*, Barcelona, 155-160. June 30 - July 3.

Odgaard, P. F., Stoustrup, J. & Kinnaert, M. 2013. Fault-Tolerant Control of Wind Turbines: A Benchmark Model. *IEEE Trans. on Control Systems Technology,* 21, 4, 1168-1182.

Sami, M. 2012. *Active Fault-Tolerant Control of Nonlinear Systems with Wind Turbine Application.* Ph.D. Thesis, The University of Hull.

Sami, M. & Patton, R. J. 2012a. Fault tolerant adaptive sliding mode controller for wind turbine power maximisation. 7th IFAC Symposium on Robust Control Design, Aalborg Congress & Culture Centre, Denmark, 499-504. 20-22 Jun.

Sami, M. & Patton, R. J. 2012b. Wind turbine power maximisation based on adaptive sensor fault tolerant sliding mode control. 20th Mediterranean Conference on Control & Automation, Barcelona, 1183-1188. 3-6 July.

Simani, S. & Castaldi, P. 2013a. Active actuator fault-tolerant control of a wind turbine benchmark model. *Int. J. of Robust and Nonlinear Control,* doi: 10.1002/rnc.2993.

Simani, S. & Castaldi, P. 2013b. Data-driven and adaptive control applications to a wind turbine benchmark model. *Control Engineering Practice,* 21, 12, 1678-1693.

Sloth, C., Esbensen, T. & Stoustrup, J. 2011. Robust and fault-tolerant linear parameter-varying control of wind turbines. *Mechatronics,* 21, 4, 645-659.

Stewart, G. & Lackner, M. 2013. Offshore Wind Turbine Load Reduction Employing Optimal Passive Tuned Mass Damping Systems. *IEEE Trans. on Control Systems Technology,* 21, 4, 1090-1104.

Tanaka, K. & Wang, H. O. 2001. *Fuzzy Control Systems Design and Analysis: A Linear Matrix Inequality Approach*, John Wiley.

Verbruggen, T. W. 2003. Wind turbine operation and maintenance based on condition monitoring. Energy Research Center of the Netherlands, Technical Report ECN-C-03-047.

Wei, X. & Liu, L. 2010. Fault estimation of large scale wind turbine systems. Proceedings of the 29th Chinese Control Conference, 4869-4874. 29-31 July.

Zhang, K., Jiang, B. & Cocquempot, V. 2008. Adaptive Observer-based Fast Fault Estimation. *Int. J. of Control, Automation, & Systems,* 6, 3, 320-326.